Proceedings of the
46th IEEE Conference on Decision and Control
New Orleans, LA, USA, Dec. 12-14, 2007

Using distributed magnetometers to increase IMU-based velocity estimation into perturbed area

David Vissière, Alain Martin, Nicolas Petit

Abstract— **We address the problem of position estimation for a rigid body using an inertial measurement unit (IMU) and a set of spatially distributed magnetometers. We take advantage of the magnetic field disturbances usually observed indoors. This is particularly relevant when GPS is unavailable (e.g. during military operations in urban areas). We illustrate our technique with several experimental results obtained with a Kalman filter. We also present our testing bench which consists of low cost sensors (IMU and magnetometers).**

INTRODUCTION

Numerous military and civilian control applications require high accuracy position, speed, and attitude estimations of a solid body. Examples range from Unmanned Air Vehicles (UAV), Unmanned Ground Vehicles (UGV), full-sized submarines, sub-sea civil engineering positioning devices [10], to name a few. A widely considered solution is to use embedded Inertial Measurement Units (IMU). Accelerometers, gyroscopes (and possibly magnetometers) signals can be used to derive position information through a double integration process [5], [4]. Because of sensors drifts, this approach requires very high precision IMUs Other solutions need to be used when cost, space, or weight constraints become stringent. A recent trend has been to heavily rely on the well known Global Positioning system (GPS) technology. has a limited availability (especially in the context of military operations), its accuracy is (roughly speaking) of 10 m of error. GPS is very poorly useable between buildings in forests or indoor. The recent progress in very low cost (less than 1,500 USD), low weight (less than 100 g) and low size (less than 3 cm^2) IMUs have spurred a broad interest in the development of IMU-based positioning technologies. These Micro-Electro-Mechanical Systems (MEMS) IMUs appear to have quickly increasing capabilities. Several manufacturers are announcing new models under 5,000 USD with gyroscopes capable of less than 20 deg/hr.

So far, there does not exist any reported experiment of successful position estimation from such a low cost IMU. In the literature, these IMUs are only used for attitude estimation (see e.g. [3], [7] or [2] for an application to the control of mini-UAVs in closed loop). Some tentative work (using higher-end IMUs) address the problem of velocities estimation. In these cases, the speed information is obtained from a GPS receiver using the Doppler effect (see [5] for details on the quality of the obtained measurements information) or from odometers (in the case of ground vehicles). Our focus is on indoor missions involving humans. It is desired to remotely estimate their positions. During preliminary tests, it quickly appeared to us that, given the poor knowledge of the body dynamics, it is impossible to get a position error below 50 m from a low cost IMU (e.g. a 3DMGX1 from Microstrain®) after a few minutes of experiments. For the specific problem of pedestrian indoor navigation, technical solutions exist in both academia [8], and industry (e.g. Core Navigation Module by Vectronix®). These methods do not rely on velocity inertial estimates, but, rather, evaluate step lengths and walking pace. An IMU is used to provide heading information, and to detect stop and go sequences. Obtained results are good, provided that the pedestrian is not walking side ways, and keeps a regular step length. It is also required that the magnetic field is not disturbed. High-end IMUs are usually much too heavy for human-oriented applications. While the GPS signal is poorly available indoor, experimental measurements have shown that the magnetic field in a typical business building is strongly disturbed (by the building structure, electrical equipments and computers among others). For sake of illustration, we report the variations of the magnetic field norm inside a business building office in Figure 2.

Our claim is that these disturbances (which are assumed to

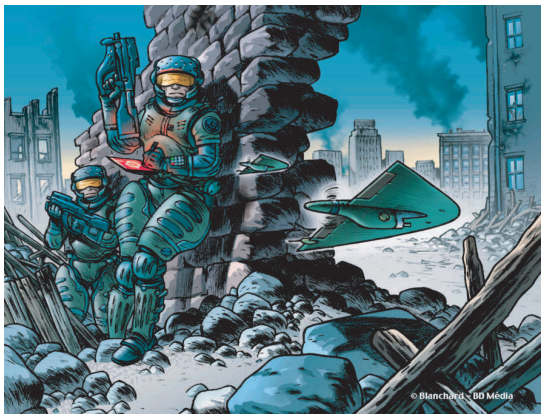

Fig. 1. A typical platoon of soldiers in action as envisioned in the BOA projet.©F.Blanchard-BD Médias for Délégation Générale pour l'Armement (DGA). A team leader keeps track of his soldiers thanks to real-time position information reported on his arm held display.

D. Vissière (corresponding author) is "Ingénieur de l'Armement" in the Délégation Générale pour l'Armement (DGA) of the French Department of Defense. He is a PhD candidate in Mathematics and Control, Centre Automatique et Systèmes, École des Mines de Paris, 60, bd St Michel, 75272 Paris, France david.vissiere@dga.defense.gouv.fr

A. Martin is "Ingénieur" in the Délégation Générale pour l'Armement (DGA) of the French Department of Defense.

N. Petit is with the Centre Automatique et Systèmes, École Nationale Supérieure des Mines de Paris, 60, bd St Michel, 75272 Paris, France

1-4244-1498-9/07/$25.00 ©2007 IEEE.

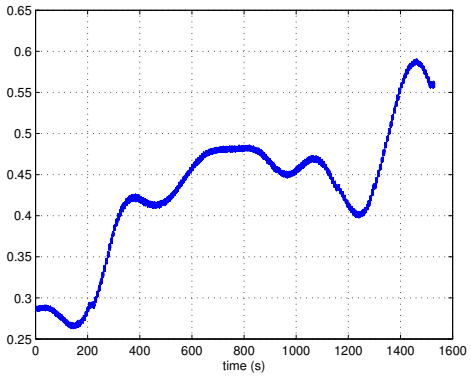

Fig. 2. Variation of the magnetic field norm during a 2.4 m horizontal displacement inside a business building office.

be stationary) can actually be used to improve the position estimation. Our work is related to the approach advocated in [6] for gravimetry aided navigation. Very importantly, our approach does not rely on any a-priori magnetic map. It simply uses Maxwell's equation. In words, we note that, in a disturbed magnetic field, it is possible to determine when a solid body equipped with 4 magnetometers is moving. If it moves, then the sensed magnetic fields must change in accordance with Maxwell's law. If the magnetic measurements do not change significantly, then the solid body is not moving. This allows us to rule out velocity drifts from the estimation. Eventually, this improves the position information obtained by integrating the velocity estimate. In [11], we proposed, in a first approach, to model the magnetic field spatial derivatives with low pass dynamics driven by white noises. Here, we use an orthogonal trihedron of magnetometers, to directly measure these derivatives and reconciliate magnetic and inertial information. The experimental results that we present lead us to believe it is possible to estimate the position of a man who is investing a building while bearing a low cost package consisting of an IMU and 3 additional magnetometers . This objective fits in the *network centric warfare* (as defined in [9]) context "Bulle Opérationnelle Aéroterrestre" (BOA), led by the Délégation Générale pour l'Armement (DGA) for the French Department of Defense. A typical mission in the BOA environment is depicted in Figure 1.

The article is organized as follows. In Section I, we define the position estimation problem. Notations required for the study of the dynamics are presented. In Section II, we expose our use of magnetic disturbances and sensors. In particular, in that case, we prove the observability of the velocity. In Section III, we present experimental results, discuss implementation details, and comment on the calibration issues. Finally, in Section IV, we conclude and suggest several directions of improvement.

I. Problem statement

In this section, we present the equation of motion of a rigid body, the various frames under consideration, and the measurement equations from available sensors (namely gyroscopes, accelerometers and magnetometers).

A. Coordinate frames, system of equations, notations

An IMU (viewed as a material point) is located at the center of gravity of a moving body we desire to estimate the position of. This six degrees of freedom system can simultaneously rotate and translate. A body-fixed reference frame with origin at the center of gravity of the IMU is considered. In the following, subscript $_b$ refers to this body frame. The x, y and z axis are the IMU axis (i.e. are consistent with the inner sensors orientations).

As inertial reference frame, we consider the local frame. It corresponds to the North-East-Down frame when initial heading is zero: NED, the X axis is tangent to the geoid and is pointing to the north, the Z axis is pointing to the center of the Earth, and the Y axis is tangent to the geoid and is pointing to the East. Subscript $_i$ refers to this inertial frame.

The IMU delivers a 9 parameters vector $[Y_V \quad Y_\Omega \quad Y_{M_0}]^T$ obtained from a 3-axis accelerometer, a 3-axis gyroscope and a 3-axis magnetometer. Measurements are noisy and biased. Classically, we consider that the accelerometer signal Y_V has a bias B_V (independently on each axis) and suffers from additive white noise $\mu_v \in \mathbb{R}^3$, and that both the magnetometer signal Y_{M_0} and the gyros signal Y_Ω have additive white noises $\mu_M \in \mathbb{R}^3$ and $\mu_\Omega \in \mathbb{R}^3$, respectively. Finally, there is a drift $B_\Omega \in \mathbb{R}^3$ on Y_Ω. It is possible to consider unknown scale factors to increase filtering accuracy, but these are not necessary in a first approach. We note $B_V \in \mathbb{R}^3$ the drift of the accelerometer and $B_\Omega \in \mathbb{R}^3$ the drift of the gyroscope.

The rigid body is also equipped with three external magnetometers. These deliver three 3 measurement vectors $[Y_{M_1} \quad Y_{M_2} \quad Y_{M_3}]^T$. Each magnetometer has its own unknown scale factor, bias, and misalignment angles. To use these signals, it is necessary to precisely obtain good estimates of these unknown parameters. A calibration procedure is presented in Section III.

Noting F the external forces (excluding gravity) acting on the IMU, and R the rotation matrix from the inertial frame to the body frame, we can write the measurement equations from the IMU as $Y = [Y_V \quad Y_\Omega \quad Y_{M_0}]^T$ with

$$\left.\begin{aligned} Y_V &= F - R\vec{g} + B_V + \mu_V \\ Y_\Omega &= \Omega + B_\Omega + \mu_\Omega \\ Y_{M_0} &= M + \mu_{M_0} \end{aligned}\right\} \quad (1)$$

where $\vec{g}$ stands for the gravity vector with norm g, and M is the magnetic field in the body frame. For the bias vector $B = [B_V \quad B_\Omega]^T$, several models can be considered depending on accuracy requirements. A second order damped oscillator driven by a white noise is a good choice. Classically, in filter equations, bias will be treated in an extended state.

From a dynamical system point of view, the state of the rigid body is described by the 12 following independent variables.

- $X = [x \quad y \quad z]^T$ is the position of the center of gravity of the IMU in the inertial frame

- $V = [u \quad v \quad w]^T$ is the vector velocity of the center of gravity of the IMU in the body frame
- $Q = [\phi \quad \theta \quad \psi]^T$ stands for the Euler angles, i.e. the angles between the inertial frame and the body
- $\Omega = [p \quad q \quad r]^T$ are the angular rates.

The input vector of the dynamics are the forces $F = [F_u \quad F_v \quad F_w]^T$ and torques. We call R the rotation matrix from the inertial frame to the body frame.

$$R = \begin{bmatrix} c\psi c\theta & s\psi c\theta & -s\theta \\ -c\phi s\psi + s\phi s\theta c\psi & c\phi c\psi + s\phi s\psi s\theta & c\theta s\phi \\ s\phi s\psi + c\phi s\theta c\psi & -s\phi c\psi + c\phi s\psi s\theta & c\theta c\phi \end{bmatrix}$$

with the notations $c* = \cos(*)$, $s* = \sin(*)$.

Remark: To avoid the well known singularities when θ reaches $\pm\frac{\pi}{2}$, quaternions can be used to represent the Euler angles. For sake of simplicity, we do not present quaternions equations but they are handy in this situation, and useful to implement the filter equations.

B. Equations of motion

The matrix of inertia of the system is unknown. It is approximated by the identity matrix. Models for the unknown forces F and angular rates Ω dynamics must be chosen. A very basic choice is to model them with white noises. Implicitly, the variance of the white noises ν_Ω and ν_F is used to specify the manoeuvring capabilities of our system. In summary, using the matrix R, we get the following system dynamics

$$\left.\begin{aligned} \dot{X} &= R^T V \\ \dot{V} &= -\Omega \times V + F \\ \dot{Q} &= G(\Omega, Q) \\ \dot{\Omega} &= \nu_\Omega \\ \dot{F} &= \nu_F \end{aligned}\right\} \tag{2}$$

with

$$G(\Omega, Q) = \begin{bmatrix} p + (q\sin(\phi) + r\cos(\phi))\tan(\theta) \\ q\cos(\phi) - r\sin(\phi) \\ (q\sin(\phi) + r\cos(\phi))\cos(\theta)^{-1} \end{bmatrix}$$

II. Using magnetic field disturbances to observe the velocity

Naturally, the measurements are expressed in the body frame. The magnetic field M is obtained through the relation

$$M = RM_i \tag{3}$$

The usual way to take the magnetic measurements into account in attitude or position estimation techniques is to consider it gives a direct measure of the heading vector. This approach gives very good results, *provided magnetic disturbances are negligible*. Yet, as can be seen in Figure 2 and Figure 3, these disturbances are not negligible indoor, e.g. in typical business offices or houses.

In the inertial frame, the following three properties can be derived from Maxwell's equations [1].

- *The magnetic field is stationary*. According to Faraday's law of induction, in the absence of electrical sources $\frac{\partial M_i}{\partial t} = 0$. In other words, the magnetic field is a function of the position only. We note it $M_i(X)$.
- *The magnetic field is a potential field*. According to Ampère's law, in the absence of electric and magnetic sources, $\mathrm{curl}(M_i) = 0$. Therefore, there exists a scalar function $h(X)$ such that $M_i = \nabla h$.
- *The divergence of the magnetic field is zero*: $\mathrm{div}(M_i) = 0$. Thanks to the previous property, this implies $\Delta h = h_{xx} + h_{yy} + h_{zz} = 0$.

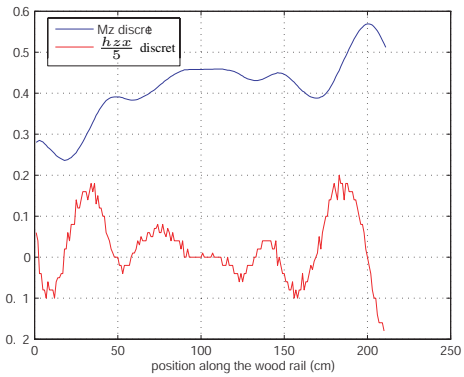

Fig. 3. Histories of h_{zx} the partial derivative of the z component of the magnetic field in the x inertial direction during a 2.1 m move at constant speed along a wood (therefore non-magnetic) rail.

In the body frame, one can differentiate (3) to get the following differential equation (thanks to a chain rule)

$$\dot{M} = -\Omega \times M + R\nabla^2 h R^T V \tag{4}$$

In [11], we considered this equation by assuming that $\nabla^2 h$ was unknown and modeled its components by first order dynamics driven by white noises ν_H. We extended the state by adding the magnetic field M and the independent gradients H. Due to the three properties presented above, there are only five independent gradients to reconstruct. These are, in the inertial frame, $H \triangleq [h_{xx} \quad h_{xy} \quad h_{xz} \quad h_{yy} \quad h_{yz}]^T \in \mathbb{R}^5$.

Some experiments have shown that strongly varying magnetic fields are difficult to estimate using this approach.

In this paper, we use a set of magnetometers to evaluate $\nabla^2 h$. Three 3-axis magnetometers are precisely mounted on a board, see Figure 4. The exact locations are defined by vector lever arms l_1, l_2, and l_3 which define a direct orthogonal trihedron. The sought after variables H are obtained from finite difference schemes. Further, we model their dynamics by a white noise

$$\dot{H} = \nu_H \tag{5}$$

Slopes depicted in Figure 3 suggest that spatial derivatives of H are not negligible. For sake of performance, it is recommended to include some higher order dynamics in both measurement and dynamics equations. For sake of simplicity, we do not present them here, but they can be easily taken into account.

Under the preceding assumptions, the vector of measurement obtained from the IMU, and the orthogonal trihedron

of magnetometers is modeled as

$$\left.\begin{array}{l} Y_V = F - Rg + B_V + \mu_V \\ Y_\Omega = \Omega + B_\Omega + \mu_\Omega \\ Y_{M_0} = M + \mu_{M_0} \\ Y_{M_1} = M + R\nabla^2 h R^T l_1 + \mu_{M_1} \\ Y_{M_2} = M + R\nabla^2 h R^T l_2 + \mu_{M_2} \\ Y_{M_3} = M + R\nabla^2 h R^T l_3 + \mu_{M_3} \end{array}\right\} \quad (6)$$

As will now appear, Equation (4) plays a key role in this observation problem. It is the only one giving direct information on V.

A. Observability

1) Linearization: In a general approach, let us consider the system obtained by linearizing the dynamics (2)-(4)-(5), and the measurement Equation (6). We denote by $\partial_X f$ the partial derivative of f with respect to X,$\partial_X f = \frac{\partial f}{\partial x}$.

From Equations (2)-(4)-(5), we obtain

$$\left\{\begin{array}{lcll} A_{XV} &=& \partial_V \dot{X}, & A_{XQ} = \partial_Q \dot{X} \\ A_{VV} &=& \partial_V \dot{V}, & A_{V\Omega} = \partial_\Omega \dot{V}, \quad A_{VF} = \partial_F \dot{V} \\ A_{QQ} &=& \partial_Q \dot{Q}, & A_{Q\Omega} = \partial_\Omega \dot{Q} \\ A_{FF} &=& 0 & \\ A_{\Gamma\Gamma} &=& 0 & \\ A_{MV} &=& \partial_V \dot{M}, & A_{MQ} = \partial_Q \dot{M}, \quad A_{M\Omega} = \partial_\Omega \dot{M} \\ A_{MM} &=& \partial_M \dot{M}, & A_{MH} = \partial_H \dot{M} \\ A_{HH} &=& 0 & \end{array}\right.$$

with

$$A_{XV} = R^T$$

$$A_{MV} = R\nabla^2 h R^T$$

$$A_{VF} = A_{Q\Omega} = A_{\Gamma\Omega} = I_3$$

$$A_{VV} = A_{MM} = \begin{bmatrix} 0 & r & -q \\ -r & 0 & p \\ q & -p & 0 \end{bmatrix}$$

$$A_{V\Omega} = \begin{bmatrix} 0 & -w & v \\ w & 0 & -u \\ -v & u & 0 \end{bmatrix}$$

$$A_{M\Omega} = \begin{bmatrix} 0 & -M_z & M_y \\ M_z & 0 & -M_x \\ -M_y & M_x & 0 \end{bmatrix}$$

$$A_{Q\Omega} = \begin{bmatrix} 1 & \sin(\phi)\tan(\theta) & \cos(\phi)\tan(\theta) \\ 0 & \cos(\phi) & -\sin(\phi) \\ 0 & \frac{\sin(\phi)}{\cos(\theta)} & \frac{\cos(\phi)}{\cos(\theta)} \end{bmatrix}$$

$$A_{QQ} = \begin{bmatrix} \frac{(qc\phi - rs\phi)s\theta}{c\theta} & \frac{qs\phi + rc\phi}{c\theta^2} & 0 \\ -qs\phi - rc\phi & 0 & 0 \\ \frac{qc\phi - rs\phi}{c\theta} & \frac{(qs\phi + rc\phi)c\theta}{\tan(\theta)} & 0 \end{bmatrix}$$

From Equation (6), we derive

$$\left\{\begin{array}{lll} C_{VQ} = \partial_Q Y_V, & C_{VF} = \partial_F Y_V & \\ C_{\Omega\Omega} = \partial_\Omega Y_\Omega & & \\ C_{M_0M} = \partial_M Y_{M_0} & & \\ C_{M_1M} = \partial_M Y_{M_1}, & C_{M_1Q} = \partial_Q Y_{M_1}, & C_{M_1H} = \partial_H Y_{M_1} \\ C_{M_2M} = \partial_M Y_{M_2}, & C_{M_2Q} = \partial_Q Y_{M_2}, & C_{M_2H} = \partial_H Y_{M_2} \\ C_{M_3M} = \partial_M Y_{M_3}, & C_{M_3Q} = \partial_Q Y_{M_3}, & C_{M_3H} = \partial_H Y_{M_3} \end{array}\right.$$

with $C_{VF} = C_{\Omega\Omega} = C_{M_0M} = C_{M_1M} = C_{M_2M} = C_{M_3M} = I_3$.

One can easily realize that the position X is not observable (it does not appear anywhere in the right-hand side of the dynamics). We now focus on the reduced state $[V; Q; \Omega; F; M; H]^T$.

2) Ignoring the properties of the magnetic field: When the properties of the magnetic field are ignored, a linear system $\dot{\Sigma} = A\Sigma$, $\Delta Y = C\Sigma$ is obtained from the preceding linearization. The state vector is $[V; Q; \Omega; F]^T \in \mathbb{R}^{12}$. Matrices A and C are, respectively,

$$A = \begin{bmatrix} A_{VV} & 0 & A_{V\Omega} & A_{VF} \\ 0 & A_{QQ} & A_{Q\Omega} & 0 \\ 0 & 0 & 0 & 0 \\ 0 & 0 & 0 & 0 \end{bmatrix}$$

$$C = \begin{bmatrix} 0 & C_{VQ} & 0 & C_{VF} \\ 0 & 0 & C_{\Omega\Omega} & 0 \end{bmatrix}$$

When computing the observability matrix $\mathcal{O} = \begin{bmatrix} C; & CA; & CA^2; & ...; & CA^{11} \end{bmatrix}$, one easily realizes that its first column is identically equal to zero. In fact, the rank of $\mathbb{O}$ is

$$rank[\mathcal{O}] = rank[C_{VQ}A_{QQ}] + rank[C_{VF}] + rank[C_{\Omega\Omega}] = 8$$

When ignoring the properties of the magnetic field, it appears that V and ψ are not observable. Using only gyroscopes and accelerometers, only ϕ, θ, Ω, and F can be observed.

3) Accounting for the properties of the magnetic field: In this setup, we consider the full state $[V; Q; \Omega; F, M, H]^T \in \mathbb{R}^{20}$. We obtained another linear system $\dot{\Sigma} = A\Sigma$, $\Delta Y = C\Sigma$ with

$$A = \begin{bmatrix} A_{VV} & 0 & A_{V\Omega} & A_{VF} & 0 & 0 \\ 0 & A_{QQ} & A_{Q\Omega} & 0 & 0 & 0 \\ 0 & 0 & 0 & 0 & 0 & 0 \\ 0 & 0 & 0 & 0 & 0 & 0 \\ A_{MV} & A_{MQ} & A_{M\Omega} & 0 & A_{MM} & A_{MH} \\ 0 & 0 & 0 & 0 & 0 & 0 \end{bmatrix}$$

$$C = \begin{bmatrix} 0 & C_{VQ} & 0 & C_{VF} & 0 & 0 \\ 0 & 0 & C_{\Omega\Omega} & 0 & 0 & 0 \\ 0 & 0 & 0 & 0 & C_{MM} & 0 \\ 0 & C_{M_1Q} & 0 & 0 & C_{MM} & C_{M1_H} \\ 0 & C_{M_2Q} & 0 & 0 & C_{MM} & C_{M2_H} \\ 0 & C_{M_3Q} & 0 & 0 & C_{MM} & C_{M3_H} \end{bmatrix}$$

The observability matrix is $\mathcal{O} = \begin{bmatrix} C; & CA; & CA^2; & ...; & CA^{19}; \end{bmatrix}$. In its first column, a term appears, namely A_{MV} (which corresponds to the partial derivative of the magnetic fields with respect to the velocity V). In details,

$$rank[\mathcal{O}] \geq rank[A_{MV}] + rank\begin{bmatrix} C_{VQ} \\ A_{MQ} \end{bmatrix} + rank[C_{\Omega\Omega}]$$
$$+ rank[A_{MV}A_{VF}] + rank[C_{MM}] + rank\begin{bmatrix} C_{M_1H} \\ C_{M_2H} \\ C_{M_3H} \end{bmatrix}$$

As proven in the Appendix, $\mathcal{O}$ is full rank (20) under the following conditions:

- $|\theta| < \frac{\pi}{2}$
- $\nabla^2 h$ is invertible
- $\nabla^2 h$ is not of the diagonal form $diag(a, a, -2a), a \in \mathbb{R}$ and at least one of the first two components of $R_\theta^T R_\phi^T V$ is non zero.

If the last condition is not satisfied, then $rank(\mathcal{O}) = 19$ and the non observable state is ψ. It is possible to get some physical insight into these conditions: the first two components of $R_\theta^T R_\phi^T V$ correspond (up to a R_ψ rotation) to the coordinates of the velocity vector in the inertial frame (x, y)-plane. At least, one of these has to be non zero, so that ψ can be recovered. Also, if the $\nabla^2 h$ is of the mentioned diagonal form, then the magnetic disturbances are insufficient to recover the heading variable.

III. Filter design and experimental results

Thanks to the discussed observability property of the system (2)-(4)-(5)-(6), we implemented an extended Kalman filter (EKF) to reconstruct the state $[V; Q; \Omega; F, M, H]^T \in \mathbb{R}^{20}$, and, eventually, use it to estimate the position $X \in \mathbb{R}^3$.

A. Filter design

In practice, the state of our EKF is composed of 45 variables including configuration states (12 variables), magnetic field and its independent first and second derivatives (3+5+7 variables), forces and torques (3+3 variables), sensors biases (6 variables). We used equally valued tuning parameters for the 3 axis. These are chosen to capture fast dynamics ($\sigma_{acceleration} = 8$ m.s^{-2}, $\sigma_{torque} = 4$ rad.s^{-2}). Classically, discrete-time updates are implemented. Updates are synchronized with the 75Hz measurements from the IMU.

The EKF states X evolves according to the following continuous time model $\dot{X} = F(X, U)$ where U is the input variable.

First, a prediction from time k to $k+1$ is performed, this gives X_p and P_p , and then the EKF estimates the state from the measurements, yielding X_e and P_e. We note T the sampling time, Q and R being the covariances matrix of the zero-mean dynamic and sensors white noises, respectively. The updates are computed as follows:

$$
\begin{aligned}
X_p &= X_e + F(X_e, U)T \\
P_p &= (I + AT)P_e(I + AT)^T + QT + (AQ + QA^T)\frac{T^2}{2} \\
&\quad + AQA^T\frac{T^3}{3} \\
Y_p &= [F - Rg + B_V; \Omega + B_\Omega; M; M + R\nabla^2 h R^T l_1; \\
&\qquad M + R\nabla^2 h R^T l_2; M + R\nabla^2 h R^T l_3]^T \\
K &= P_p C^T (R + C P_p C^T)^{-1} \\
X_e &= X_p + K(Y - Y_p) \\
P_e &= (I - KC)P_p(I - KC)^T + KRK^T
\end{aligned}
$$

B. Experimental testing bench and calibration issues

1) Testing bench:: Our experimental testing bench is designed to illustrate the relevance of our approach in standard buildings inside which the magnetic field is unknown and has significant 3-dimensional variations. Off the shelves IMUs are used (e.g. a 3DMGX1 from Microstrain®)

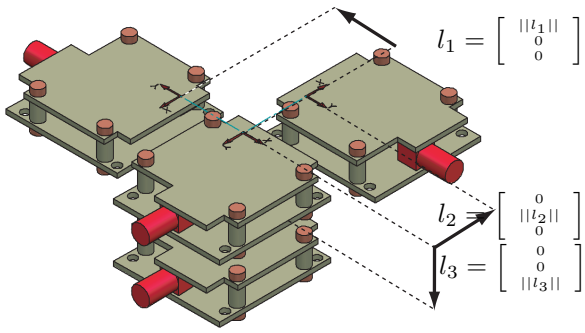

Fig. 4. Experimental testing bench with the four IMU, one giving accelerations,raw data, magnetic field and the three other used as simple external magnetometers

Four IMUs are fixed on a board which can simultaneously rotate and translate in 3D. Only one out of the four is actually used as an IMU. The remaining three are used as 3-D magnetometers. This board has been used in different rooms in our building. Obtained results are very similar.

2) Calibration issues: While the four IMU are supposed to be very similar, experimentally, a serious practical issue is sensors calibration. Even if mechanical tolerances are indeed small, we quickly realized that it was absolutely necessary to determine bias, misalignment angles, and scale factors for every magnetometer. Each magnetometer measurement is modeled as follows, for $j, (j = 0...3)$,

$$
\begin{aligned}
Y_{jm} &= \alpha_j R_j Y_j + \beta_j \quad \text{with } \beta = [\beta_{j1}\ \beta_{j2}\ \beta_{j3}]^T \\
R_j &= \begin{bmatrix} 1 & \psi_j & -\theta_j \\ -\psi_j & 1 & \phi_j \\ \theta_j & -\phi_j & 1 \end{bmatrix} \alpha_j = \begin{bmatrix} \alpha_{j1} & & \\ & \alpha_{j2} & \\ & & \alpha_{j3} \end{bmatrix}
\end{aligned}
$$

The small scale of possible measurements (± 1 G)prevents us from using comparisons with a calibrated induction. Rather, we compute the unknown parameters α_j, β_j and R_j as the minimizers of a least square problem under the constraints that the reconstructed vector $(hxx, hxy, hxz, hyx, hyy, hyz, hzx, hzy, hzz)$ must define a symmetric Hessian $\nabla^2 h$ with zero trace. A large number of experimental data was used to define this least square problem.

C. Experimental results

We consider the following normalized experiment. Sequentially, the board is moved forward along a 1 m straight line in 10 cm steps. This motion is accurately measured. No a priori information about the trajectory is given to the filter. Data are transferred to a remote PC and treated off-line. For sake of comparisons, we present position estimation results obtained with three different methods. The first one is presented here, it uses the four magnetometers. The second method was presented in [11]. As already discussed, it uses a single magnetometer. Finally, results obtained with inertial

calculations (using only gyroscopes and accelerometers) are presented.

For each conducted experiment, we expose speed and position estimates histories. Blue plots refer to the x-axis, green plots refer to the y-axis and red plots refer to the z-axis.

Ignoring the magnetometers, position estimates diverge over time see Figure 5(e). The filter can not get rid of errors in velocities.

Using a single magnetometer, we obtain much better results. This time, velocities, reported in Figure 5(c), remain close to zero when the IMU is at rest. This prevents the position estimates from diverging.

Most interestingly, when using the four magnetometers, we improve the accuracy a lot. Results are reported in Figure 5(a)(b). Errors in positions fall under ± 2 cm.

IV. Conclusions and future directions

In this paper, we improve upon our previously obtained results. Considering, as we did in [11], Equation (4), we reconciliate the velocity estimate and the magnetic field disturbances. Compared to our original approach, we designed and used an experimental orthogonal trihedron of four magnetometers, which gives, through finite difference schemes, a direct measurement of the magnetometer field spatial partial derivatives.

Accurate calibration of the sensors is a key issue that remains to be explored further, it can be improved upon using second order centered schemes. Real time implementation is double using a PC laptop running Matlab. The computational requirements can be reduced by neglecting some non crucial states in the EKF. We carried out some experiments, reported in Figure 5, to quantitatively Compare the improvement over other methods.

Finally, we would like to give some preliminary 3-D experimental results. Measuring this 3-D displacement requires some specific instrumentation, that could not be used yet. Quantifying the obtained accuracy remains to be done, but the results seem positive. During this experiment, the rigid body was moved (sequentially) along the three axis of an orthogonal trihedron. This motion is easily recognizable in Figure 6.

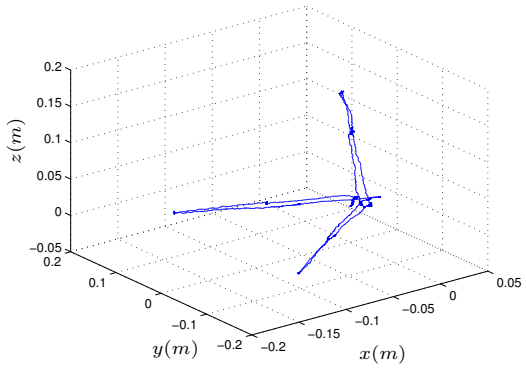

Fig. 6. The body is sequentially moved along the three axis of an orthogonal trihedron, position estimates are reported

References

[1] R. Abraham, J. E. Marsden, and T. Ratiu. *Manifolds, Tensor Analysis, and Applications*. Springer, second edition, 1988.

[2] P. Castillo, A. Dzul, and R. Lozano. Real-time stabilization and tracking of a four rotor mini rotorcraft. *IEEE Trans. Control Systems Technology*, 12(4):510–516, 2004.

[3] S. Changey, D. Beauvois, and V. Fleck. A mixed extended-unscented filter for attitude estimation with magnetometer sensor. In *Proc. of the 2006 American Control Conference*, 2006.

[4] P. Faurre. *Navigation inertielle et filtrage stochastique*. Méthodes mathématiques de l'informatique. Dunod, 1971.

[5] M. S. Grewal, L. R. Weill, and A. P. Andrews. *Global positioning systems, inertial navigation, and integration*. Wiley Inter-science, 2001.

[6] C. Jekeli. Precision free-inertial navigation with gravity compensation by an onboard gradiometer. *J. Guidance, Control and Dynamics*, 29(3):704–713, 2006.

[7] R. Mahony, T. Hamel, and J.-M. Pflimlin. Complementary filter design on the special orthogonal group SO(3). In *Proc. of the 44th IEEE Conf. on Decision and Control, and the European Control Conference 2005*, 2005.

[8] O. Mezentsev, G. Lachapelle, and J. Collin. Pedestrian dead reckoning a solution to navigation in GPS signal degraded areas? *GEOMATICA*, 59(2), 2005.

[9] Department of Defense. Network centric warfare. Technical report, Report to Congress, 2001.

[10] R. Sabri, C. Putot, F. Biolley, C. Le Cunff, Y. Creff, and J. Lévine. Automatic control methods for positioning the lower end of a filiform structure, notably an oil pipe, at sea. U.S. Patent 7,066,686, Institut Francais du Pétrole, 2006.

[11] D. Vissiere, A. Martin, and N. Petit. Using magnetic disturbances to improve IMU-based position estimation. In *Proc. of the 9th European Control Conf.*, 2007.

Appendix

We wish to compute the observability matrix $\mathcal{O} = [C; CA; ...; CA^{19}]$ with C and A defined in Section III. $\mathcal{O}$ is given in Equation (7). Bold elements (in brackets) play a key role in the rank computation. We have seen that

$$rank[\mathcal{O}] = rank[A_{MV}] + rank\begin{bmatrix} C_{VQ} \\ A_{MQ} \end{bmatrix} + rank[C_{\Omega\Omega}]$$
$$+rank[A_{MV}A_{VF}] + rank[C_{MM}] + rank\begin{bmatrix} C_{M_1H} \\ C_{M_2H} \\ C_{M_3H} \end{bmatrix}$$

We now study each of these terms.

First, $rank[A_{MV}] = 3$, provided that $\nabla^2 h$ is invertible. Then, as is proven in Proposition 2, $rank\begin{bmatrix} C_{VQ} \\ A_{MQ} \end{bmatrix} = 3$. Simply, $rank[C_{\Omega\Omega}] = 3$. Provided that $\nabla^2 h$ is invertible, $rank[A_{MV}A_{VF}] = rank[A_{MV}] = 3$. Directly, $rank[C_{MM}] = 3$. And finally, $rank\begin{bmatrix} C_{M_1H} \\ C_{M_2H} \\ C_{M_3H} \end{bmatrix} = 5$, as is proven in Proposition 1.

Proposition 1: $rank\begin{bmatrix} C_{M_1H} \\ C_{M_2H} \\ C_{M_3H} \end{bmatrix} = 5$

Proof: Let us now consider the measurement equation (6) for the four magnetometers. We note the lever arm in the inertial frame for each magnetometer j by $lj_i =$

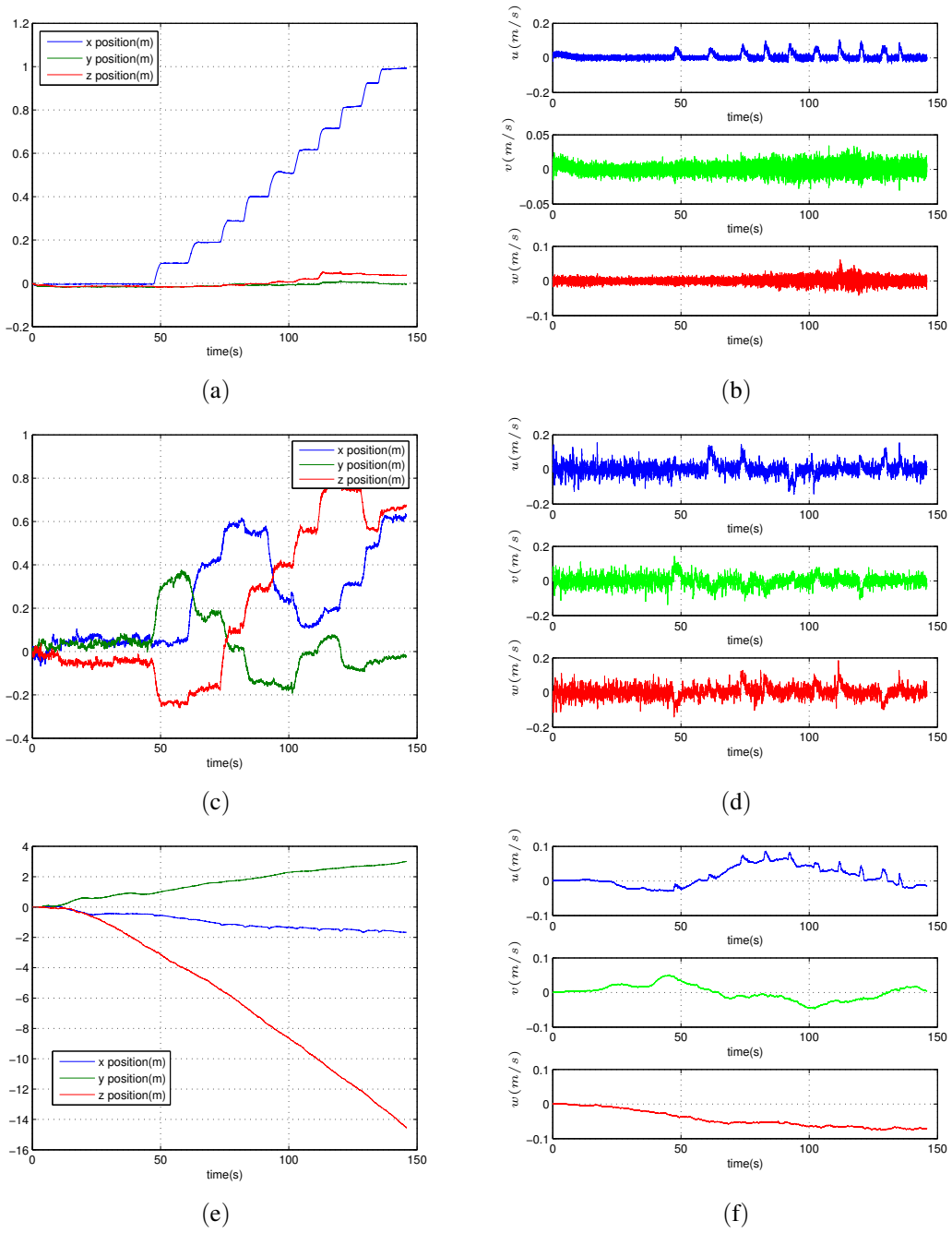

Fig. 5. Succession of steps when the experimental testing bench is horizontal. Three methods are compared. Top: using the presented four magnetometers method. Middle: using a single magnetometer. Bottom: without magnetometer. Position estimates (a),(c),(e). Velocity estimates (b), (d), (f)

$[lj_{xi}\ lj_{yi}\ lj_{zi}]^T = R^T l_j$. Considering the j^{th}, magnetometer we get

$$C_{M_j H} = \frac{\partial R \nabla^2 h R^T l_j}{\partial H}$$
$$= R\frac{\partial}{\partial H}\left(\begin{bmatrix} hxx & hxy & hxz \\ hxy & hyy & hyz \\ hxz & hyz & -(hxx+hyy) \end{bmatrix}\begin{bmatrix} lj_{xi} \\ lj_{yi} \\ lj_{zi} \end{bmatrix}\right)$$
$$= R\begin{bmatrix} lj_{xi} & lj_{yi} & lj_{zi} & 0 & 0 \\ 0 & lj_{xi} & 0 & lj_{yi} & lj_{zi} \\ -lj_{zi} & 0 & lj_{xi} & -lj_{zi} & lj_{yi} \end{bmatrix}$$

Yet, $rank\begin{bmatrix} C_{M_1 H} \\ C_{M_2 H} \\ C_{M_3 H} \end{bmatrix} = rank\begin{bmatrix} R^T C_{M_1 H} \\ R^T C_{M_2 H} \\ R^T C_{M_3 H} \end{bmatrix}$. This last

$$\mathcal{O} = \begin{bmatrix} 0 & [\mathbf{C_{VQ}}] & 0 & C_{VF} & 0 & 0 \\ 0 & 0 & [\mathbf{C_{\Omega\Omega}}] & 0 & 0 & 0 \\ 0 & 0 & 0 & 0 & [\mathbf{C_{MM}}] & 0 \\ 0 & C_{M_1Q} & 0 & 0 & C_{MM} & [\mathbf{C_{M_1H}}] \\ 0 & C_{M_2Q} & 0 & 0 & C_{MM} & [\mathbf{C_{M_2H}}] \\ 0 & C_{M_3Q} & 0 & 0 & C_{MM} & [\mathbf{C_{M_3H}}] \\ 0 & C_{VQ}A_{QQ} & C_{VQ}A_{Q\Omega} & 0 & 0 & 0 \\ 0 & 0 & 0 & 0 & 0 & 0 \\ A_{MV} & [\mathbf{A_{MQ}}] & A_{M\Omega} & 0 & A_{MM} & A_{MH} \\ [\mathbf{A_{MV}}] & C_{M_1Q}A_{QQ} + A_{MQ} & C_{M_1Q}A_{Q\Omega} + A_{M\Omega} & 0 & A_{MM} & A_{MH} \\ A_{MV} & C_{M_2Q}A_{QQ} + A_{MQ} & C_{M_2Q}A_{Q\Omega} + A_{M\Omega} & 0 & A_{MM} & A_{MH} \\ A_{MV} & C_{M_3Q}A_{QQ} + A_{MQ} & C_{M_3Q}A_{Q\Omega} + A_{M\Omega} & 0 & A_{MM} & A_{MH} \\ 0 & * & * & 0 & * & * \\ 0 & * & * & 0 & * & * \\ * & * & * & [\mathbf{A_{MV}A_{VF}}] & * & * \end{bmatrix} \quad (7)$$

matrix is, in fact,

$$\begin{bmatrix} R^T C_{M_1H} \\ R^T C_{M_2H} \\ R^T C_{M_3H} \end{bmatrix} = \begin{bmatrix} \mathbf{l1_{xi}} & \mathbf{l1_{yi}} & \mathbf{l1_{zi}} & 0 & 0 \\ 0 & l1_{xi} & 0 & \mathbf{l1_{yi}} & \mathbf{l1_{zi}} \\ -l1_{zi} & 0 & l1_{xi} & -\mathbf{l1_{zi}} & \mathbf{l1_{yi}} \\ \mathbf{l2_{xi}} & \mathbf{l2_{yi}} & \mathbf{l2_{zi}} & 0 & 0 \\ 0 & l2_{xi} & 0 & \mathbf{l2_{yi}} & \mathbf{l2_{zi}} \\ -l2_{zi} & 0 & l2_{xi} & -\mathbf{l2_{zi}} & \mathbf{l2_{yi}} \\ \mathbf{l3_{xi}} & \mathbf{l3_{yi}} & \mathbf{l3_{zi}} & 0 & 0 \\ 0 & l3_{xi} & 0 & \mathbf{l3_{yi}} & \mathbf{l3_{zi}} \\ -l3_{zi} & 0 & l3_{xi} & -\mathbf{l3_{zi}} & \mathbf{l3_{yi}} \end{bmatrix}$$

The bold elements in the three first column correspond to $(R^T[l_1 l_2 l_3])^T$ which is of rank 3, then the rank of the lines 1,4 and 7 is 3. Now let us consider the last two columns. By computing the three 2×2 determinants, we obtain: $l1_{yi}^2 + l1_{zi}^2$ for the first one and $l2_{yi}^2 + l2_{zi}^2$ and $l3_{yi}^2 + l3_{zi}^2$ for the others two. Assuming that these determinants are all zero, last conditions are exclusive. If the first one holds, then the rotation R is around the x axis. If the second holds, then the rotation R is around the z axis (with an angle of $-\pi/2$). If the third holds, then the rotation R is around the y-axis (with an angle of $\pi/2$). At least, one of the determinants must be non zero. This gives the conclusion. ■

Proposition 2: Assuming that $|\theta| < \frac{\pi}{2}$, $rank \begin{bmatrix} C_{VQ} \\ A_{MQ} \end{bmatrix} \geq 2$. Sufficient conditions for $rank \begin{bmatrix} C_{VQ} \\ A_{MQ} \end{bmatrix} = 3$ are that, at least one of the first two components of $R_\theta^T R_\phi^T V$ is non zero and that $\nabla^2 h$ is not of the form $diag(a, a, -2a), a \in \mathbb{R}$.

Proof: By definition,

$$C_{VQ} = \frac{\partial}{\partial Q}(-Rg) = g \begin{bmatrix} 0 & -\cos(\theta) & 0 \\ \cos(\theta)\cos(\phi) & -\sin(\theta)\sin(\phi) & 0 \\ -\sin(\phi)\cos(\theta) & -\sin(\theta)\cos(\phi) & 0 \end{bmatrix}$$

which always satisfy, provided $|\theta| < \frac{\pi}{2}$, $rank(C_{VQ}) = 2$. The possible extra rank may comes from the third column $A_{M\psi} = \frac{\partial M}{\partial \psi}$ of A_{MQ}:

$$\begin{aligned} A_{M\psi} &= \frac{\partial}{\partial \psi}(R\nabla^2 h R^T V) \\ &= \frac{\partial}{\partial \psi}(R_\phi R_\theta R_\psi \nabla^2 h R_\psi^T R_\theta^T R_\phi^T V) \\ &= R_\phi R_\theta \frac{\partial}{\partial \psi}(R_\psi \nabla^2 h R_\psi^T R_\theta^T R_\phi^T V) \end{aligned}$$

Note $R_\theta^T R_\phi^T V = \tilde{V}$, it follows that

$$\begin{aligned} &\{\frac{\partial}{\partial \psi}(R_\psi \nabla^2 h R_{-\psi} \tilde{V}) = 0\} \\ &\Rightarrow \{\forall (\psi_1, \psi_2) \in \mathcal{R}^2, R_{\psi_1} \nabla^2 h R_{\psi_1}^T \tilde{V} = R_{\psi_2} \nabla^2 h R_{\psi_2}^T \tilde{V}\} \end{aligned}$$

By evaluating these last conditions for particular points: $(\psi_1 = \frac{\pi}{2}, \psi_2 = 0)$,$(\psi_1 = -\frac{\pi}{2}, \psi_2 = 0)$ and $(\psi_1 = \pi, \psi_2 = 0)$, we obtain, after some calculus, that $\frac{\partial}{\partial \psi}(R_\psi \nabla^2 h R_{-\psi} \tilde{V}) = 0$ implies that either:
$(\tilde{u}, \tilde{v}) = (0, 0)$ or $\nabla^2 h$ is of the form $diag(a, a, -2a), a \in \mathbb{R}$.

Conversely, if this condition fails, then $\frac{\partial}{\partial \psi}(R_\psi \nabla^2 h R_{-\psi} \tilde{V}) \neq 0$ which concludes the proof. ■